

PowerEnergy2017-3442

METHOD TO DESIGN A HYDRO TESLA TURBINE FOR SENSITIVITY TO VARYING LAMINAR REYNOLDS NUMBER MODULATED BY CHANGING WORKING FLUID VISCOSITY

Mubarak S. Alrabie

Mechanical & Manufacturing
Engineering Dept.
Tennessee State University
Nashville, Tennessee, USA

Faisal N. Altamimi

Mechanical & Manufacturing
Engineering Dept.
Tennessee State University
Nashville, Tennessee, USA

Muhammad H. Altarrgemy

Mechanical & Manufacturing
Engineering Dept.
Tennessee State University
Nashville, Tennessee, USA

Fatemeh Hadi

Mechanical & Manufacturing
Engineering Dept.
Tennessee State University
Nashville, Tennessee, USA

Muhammad K. Akbar

Mechanical & Manufacturing
Engineering Dept.
Tennessee State University
Nashville, Tennessee, USA

Matthew J. Traum

Engineer Inc
Nashville, Tennessee, USA

ABSTRACT

There has been a recent surge in interest for Tesla turbines used in renewable energy applications such as power extraction from low-quality steam generated from geothermal or concentrated solar sources as well as unfiltered particle-laden biomass combustion products. High interest in these bladeless turbines motives renewed theoretical and experimental study.

Despite this renewed interest, no systematic Tesla turbine design process based in foundational theory has been published in the peer reviewed engineering literature. A design process is thus presented which is flexible, allowing an engineering designer to select and address goals beyond simply maximizing turbine output power. This process is demonstrated by designing a Tesla turbine where Reynolds number can be easily varied while holding all other parameters fixed. Tesla turbines are extremely sensitive to inter-disk spacing. It is therefore desirable to design the experiment to avoid turbine disassembly/reassembly between tests; this assures identical disk spacing and other parameters for all tests. It is also desirable to maintain similar working fluid mass flow rate through the turbine in all tests to minimize influence of losses at the nozzle impacting shaft power output differently across experiments.

Variation in Reynolds number over more than two orders of magnitude is achieved by creating a set of two-component working fluid mixtures of water and corn syrup. Increasing

mixture mass fraction of corn syrup achieves increased working fluid viscosity but only small increase in density with a corresponding decrease in working fluid Reynolds number.

The overall design goal is to create a turbine that allows modulating Reynolds number impact on Tesla turbine performance to be evaluated experimentally. The secondary goal is to size the turbine to maximize sensitivity to changes in Reynolds number to make experimental measurement easier.

The presented example design process results in a Tesla turbine with 8-cm-outer-diameter and 4-cm-inner-diameter disks. The turbine will be able to access a range of Reynolds numbers from $0.49 < Re_m < 99.50$. This range represents a Reynolds number ratio of $Re_{m,max}/Re_{m,min} = 202.8$, more than two orders of magnitude and spanning the lower part of the laminar range. The turbine's expected power output will be $\dot{W} = 0.47$ Watts with a delivered torque of 0.024 mN-m at a rotation rate of $\omega_{max} = 1197$ rev/min.

Combining the analytical equations underpinning the design process with similarity arguments, it is shown that shrinking the Tesla turbine's physical scale drives the Reynolds number toward 0. The resulting velocity difference between the working fluid and the turbine disks gets driven toward infinity, which makes momentum transfer and the resulting turbine efficiency extremely high. In other words, unlike conventional turbines whose efficiency drops as they are scaled down, the

performance of Tesla turbines will increase as they are made smaller.

Finally, it is shown through similarity scaling arguments that the 8-cm-diameter turbine resulting from the design process of this paper and running liquid Ethylene Glycol working fluid can be used to evaluate and approximate the performance of a 3-mm-diameter Tesla turbine powered by products of combustion in air.

INTRODUCTION

Tesla turbines (also called boundary layer turbines, disk turbines, or drag turbines) operate through a mechanism different from conventional axial turbines. In a conventional turbine, working fluid impinges upon aerodynamic blades to generate rotational force through aerodynamic momentum transfer. By contrast, Tesla turbines generate rotational force via momentum transfer through shear stresses as working fluid spirals through micro-channels created by flat, parallel, co-rotating disks. As a result, Tesla turbines have been observed to be robust against two-phase flow [1], a mixture of phases that typically cannot be introduced into conventional axial or radial turbines without ablating and damaging the aerodynamic blades [2-5]. Resulting Tesla turbine renewable energy applications include power extraction from particulate-laden wood gas as well as from low-quality two-phase flow obtained from concentrated solar, industrial heat recovery, or geothermal heat sources – applications all unsuited for conventional turbines.

Several Tesla turbine parameters are thought to (or have been shown to) impact performance, including disk spacing; disk number; disk surface roughness; number, size, and shape of nozzles; location/orientation of nozzles and exhaust ports; and working fluid thermodynamic and physical properties [6, 7]. However, little theoretical or experimental exploration of these parameters has occurred because Tesla turbines remain generally outside mainstream hydro-, gas-, and stream-turbine research. Thus, there is no generally accepted design or sizing methodology in the literature for Tesla turbines that considers these parameters. Further fueling estrangement of this important technology from mainstream research, the knowledge and capability gap for Tesla turbine design has been filled by the empirical guidelines of amateur hobbyists and not verified or understood using systematic engineering analysis [8, 9.]

To address the need for Tesla turbine design and sizing methodologies in the peer reviewed engineering literature, the goals of this paper are to 1) utilize what established Tesla turbine performance theory does exist to develop the needed methodology; 2) select a particular design goal different from the conventional desired turbine design outcome, maximized power output; and 3) apply the methodology to extract key physical and geometric turbine parameters that will be used for turbine construction and testing in a later work.

The primary design goal is *to create a Tesla turbine where a single identified parameter can be easily varied to test its performance impact on the turbine while holding all other parameters fixed*. A secondary goal is to size the turbine to

maximize sensitivity to the selected variable parameter making experimental measurement easier once the turbine is built.

To facilitate design, a predictive closed-form analytical solution for Tesla turbine rotation rate and efficiency was found in the literature [10-12] and extended into a systematic design technique that includes power output, torque, and sensitivity to variable parameters [13]. This theoretical work is applied here to the design of an experimental Tesla turbine to demonstrate the methodology and extract interesting results for discussion.

To achieve the primary design goal, the turbine will be configured so that one important parameter can be varied while the rest are held fixed. Looking forward, this approach will be used in future work to isolate and verify experimentally the turbine performance impacts of various parameters thought to be important but never systematically verified: disk spacing; disk number; disk surface roughness; number, size, and shape of nozzles; location / orientation of nozzles and exhaust ports; working fluid thermodynamic and physical properties; etc. So, which variable does an experimenter choose to modulate first?

One experimental series considered was increasing the number of turbine disks between runs to observe impact on power output. However, Tesla turbine power output is thought to be extremely sensitive to geometric variables. To add disks between runs would require turbine disassembly and reassembly between tests with no guarantee of identical fitment (especially disk spacing) between runs. So, an experimental series with increasing disk number would degrade into a precision engineering fitment problem. Instead, for a first experimental test it is desirable to vary a parameter that avoids turbine disassembly/reassembly between tests. Along similar lines, it is thought that Tesla turbine performance is sensitive to loss mechanisms at the nozzle. It is therefore desirable to maintain similar working fluid mass flow rate through the turbine in all tests to minimize variable nozzle losses across experiments.

This set of constraints makes undesirable the possibility of making geometric changes to the turbine as well as varying working fluid flow rate through it between experiments. As a result, the remaining parameter that can be varied is Reynolds number. It is known that power output of conventional small aero-derived turbines operating in the laminar range is highly sensitive to Reynolds number [14-16]. By contrast, if Tesla turbines were insensitive to Reynolds number variation, they could become a more sought after technology for power extraction scenarios where the viscosity or density (and hence Reynolds number) of working fluid changes intermittently, unpredictably, and/or uncontrollably during operation; for example, in a terrestrial solar-fired power cycle or in space-based applications where the system is rapidly cycling between solar exposure and shade [17].

With varying Reynolds number identified as the primary design objective, the secondary goal is to maximize the sensitivity of Tesla turbine output shaft power to changes in Reynolds number to facilitate easy experimental measurement. High sensitivity is achieved by taking derivatives of the turbine

model analytical power function with respect to variable parameters and finding extrema.

BACKGROUND & THEORY

The Tesla turbine was patented in 1913 [18]. Attempts exist in the hobby literature to develop closed-form analytical solutions relating geometric and working fluid parameters to Tesla turbine performance [8, 9]. Swithenbank also contributes prolifically to the hobby literature [19]. The isolated academic work of Rice and colleagues [20-24] and experiments of some others [25-34] contribute to understanding of Tesla turbine performance. A few review articles, which focus on measuring and maximizing power output, have also been published [6, 35]. This Spartan reference set constitutes the bulk of published peer reviewed Tesla turbine literature, which pales in comparison by volume and detail to the available body of work on conventional axial turbines.

A resurgent interest in Tesla turbines for their ability to process two-phase and particulate laden working fluid characteristic of renewable energy systems has sparked a number of recent theoretical studies and computational fluid dynamic (CFD) modeling [36-39]. While other candidate closed-form analytical models do exist [40], the 2010 publication by Carey [10] represents the most satisfactory baseline differentiable closed-form analytical model relating geometric and working fluid parameters to Tesla turbine performance.

This approach begins with the Navier-Stokes equations in cylindrical coordinates applied to working fluid interaction with the rotating disk of a Tesla turbine. It results in the following form for $\widehat{W}(\xi, Re_m^*)$, the dimensionless tangential velocity difference between the disk rotor and working fluid inside the turbine at any radial location,

$$\widehat{W}(\xi, Re_m^*) = \frac{e^{\frac{24\xi^2}{Re_m^*}}}{\xi} \left[\frac{Re_m^*}{24} e^{-\frac{24\xi^2}{Re_m^*}} + \widehat{W}_o - \frac{Re_m^*}{24} e^{-\frac{24}{Re_m^*}} \right] \quad (1)$$

where $\xi = r/r_o$ is a dimensionless radial disk location; \widehat{W}_o is the dimensionless relative disk/fluid velocity at the disk outer

radius ($\xi = 1$); and Re_m^* is a modified Reynolds number:

$$Re_m^* = \frac{2b\dot{m}_c}{\pi\mu r_o^2} \quad (2)$$

In addition, the turbine's efficiency (dimensionless power) is given as

$$\eta = 1 - \frac{(\widehat{W}_i + \xi_i)\xi_i}{(\widehat{W}_o + 1)} \quad (3)$$

where \widehat{W}_i is the dimensionless relative disk/fluid velocity at the exhaust ports at the disk inner radius. This baseline model was modified, as described elsewhere [13], to include expressions for torque,

$$\Gamma = \frac{\dot{W}}{\omega} \quad (4)$$

power output,

$$\dot{W} = \dot{m}(v_{\theta,o}U_o - v_{\theta,i}U_i) \quad (5)$$

and sensitivity of efficiency (dimensionless power) to variable parameters, including Reynolds number and dimensionless disk size,

$$\frac{\partial\eta}{\partial Re_m^*} = \frac{-1}{\widehat{W}_o + 1} \left\{ \frac{1}{24} - \left[\frac{24}{Re_m^{*2}} \left(\widehat{W}_o - \frac{Re_m^*}{24} \right) (\xi^2 - 1) + \frac{1}{24} \right] e^{\frac{24(\xi^2 - 1)}{Re_m^*}} \right\} \quad (6)$$

$$\frac{\partial\eta}{\partial\xi} = -\frac{\xi}{\widehat{W}_o + 1} \left[\frac{48}{Re_m^*} \left(\widehat{W}_o - \frac{Re_m^*}{24} \right) e^{\frac{24(\xi^2 - 1)}{Re_m^*}} + 2 \right] \quad (7)$$

DESIGN PROCESS

The goal of any successful engineering design process is the communication of the fully specified system to the person responsible for building it [41]. Additionally, for an experimental turbine with one variable parameter, the design process must result in a system capable of producing enough power to be easily measured while maximizing power output sensitivity with respect to the variable parameter.

To design this Tesla turbine, all variables that could be

Table 1: Pugh Chart quantitative down-selection process to viscosity and density as selected variable turbine parameters.

Customer Need → Variable Parameter ↓	Working Fluid Compatibility	Parameter Change Ease	Flat Disk Compatibility	Accommodates > 3 Disks	Disk Spacing Maintained	Experiment Size	Weighted Total
Need Importance Weight	1	5	5	3	2	3	
Inlet Diameter	3	3	5	4	2	1	62
Outlet Diameter	3	3	5	4	2	1	62
Disk Spacing	4	2	4	4	5	1	59
Disk Number	5	2	3	5	4	3	62
Fluid Viscosity & Density	5	5	5	4	5	5	<u>92</u>
Mass Flow Rate	4	5	4	4	5	4	83
Nozzle Location	3	4	2	2	1	1	44
Nozzle Number	2	5	2	3	1	2	54

modulated were identified with emphasis on physical and working fluid parameters thought to strongly influence performance. A Pugh Chart, Table 1, was populated with these parameters and engineering down-selection performed to identify the parameter best meeting experimental criteria outlined.

The conclusion emerging from this analysis was that working fluid viscosity and density together (kinematic viscosity) is the preferred parameter to vary to best meet design requirements. In the analytical model of Eq. (1), the only dimensionless variable directly influenced by viscosity and density with all other parameters fixed is Re_m^* . Therefore, the most universal way to designate varying only working fluid density and viscosity together is to describe varying Reynolds number.

To complete the design, all other unspecified turbine parameters needed to be set based on analytical model calculations: n_{disks} , r_o , r_i , t , b , h , \dot{W} , and \dot{m} . The first six are physical turbine parameters, the seventh is the needed turbine power output, and the final parameter is working fluid mass flow rate, which is set by the pump driving fluid through the turbine and fluid return loop. Externally-influenced parameters, \dot{W} and \dot{m} , were set first, and the analytical model was then used to set the physical turbine parameters to maximize turbine power sensitivity to variable kinematic viscosity.

Output Power Selection

The first parameter set was target turbine power output. A small 0.5-watt brushed DC motor will be connected to the turbine and run as a generator to provide load and produce electrical power. This power will be measured as Reynolds number is varied to determine its influence. Tesla turbines produce power at high shaft rotation rate and low torque. So, 0.5 watts was selected because it is a power large enough to be easily measureable, but it does not require a motor so large as to prevent the Tesla turbine from spinning up.

The selected motor is a Maxon A-max 12 precious metal brushed 0.5-Watt 3.0 V DC motor designed to spin at 13700 rpm at no load with a maximum torque of 0.872 mN-m in motor mode.

Working Fluid Selection

Variation in working fluid Reynolds number of over 200 times (and encompassing the lower end of the laminar flow range) with no change in mass flow rate is achieved by creating a series of two-component mixtures of two perfectly miscible fluids with dramatically different viscosities. Notably, Reynolds number could also have been affected by picking a viscous fluid and increasing its temperature between runs as was done via CFD modeling by Hasan and Benzamia [42]. However increasing working fluid temperature would also have measurably increased energy availability at the turbine inlet between runs making energy extraction comparisons more challenging. So, modulating viscosity through mixing was selected as the preferred approach. Due to its availability and

ease of use, water was selected as one of the two candidate liquids.

The second liquid must therefore be totally miscible in water and have a significantly higher viscosity. Increasing mixture mass fraction of this second fluid achieves increased working fluid viscosity with only small increase in density. A corresponding decrease in working fluid Reynolds number results. Table 2 shows the candidate fluids considered along with their key measured properties. As reliable literature values for many of these fluids' properties were difficult to find, viscosity and density were directly measured at room temperature (~ 24 °C). Viscosity was measured using a Keyu NDJ-8S Digital Rotary Viscometer, and density was measured by filling a 10 mL graduated cylinder and weighing on an Ohaus Scout Pro digital balance.

Table 2: Measured viscosity and density of candidate fluids added in a binary mixture with water to facilitate Reynolds number modulation of Tesla turbine working fluid.

Measured Parameters	Temperature [°C]	Viscosity [kg m ⁻¹ s ⁻¹]	Density [kg m ⁻³]
Water	24	0.0010	1007
Ethylene Glycol	24	0.0019	1095
Propylene Glycol	24	0.0036	1022
Fructose Syrup (Maple Syrup)	24	0.953	1356
Glucose Syrup [Corn Syrup]	24	4.400	1383
Sucrose Syrup [Molasses]	24	6.919	1458

For modeling purposes, binary mixture viscosity was estimated via the Refutas equation technique [43]. Using the kinematic viscosity (in centistokes) at the mixture temperature, the viscosity blending number (VBN) of each component is calculated,

$$VBN_i = 14.534 \times \ln[\ln(v_i + 0.8)] + 10.975 \quad (8)$$

The mixture VBN is then calculated via multiplication by mixture component mass fraction,

$$VBN_{mixture} = (x_A \times VBN_A) + (x_B \times VBN_B) \quad (9)$$

Finally, the kinematic viscosity of the mixture is extracted by inverting the VBN algorithm.

$$v_{mixture} = \exp \left[\exp \left(\frac{VBN_{mixture} - 10.975}{14.534} \right) \right] - 0.8 \quad (10)$$

Based on its relatively high viscosity, economical commercial availability in large batches, experimentally-measured physical property batch-to-batch consistency, and availability of references to estimate and model its viscosity [44], Glucose syrup (corn syrup) was selected as the second components in the variable viscosity binary mixture.

During future turbine experiments, working fluid mixture properties will be measured quickly and accurately right before tests using the Keyu NDJ-8S Digital Rotary Viscometer. These well-characterized mixtures will then be pumped through the Tesla turbine at a predetermined mass flow rate, which is set by power input to the pump. At the end of each experiment, fluid properties will again be measured to account for any drift arising from temperature change, mixture component evaporation, and/or chemical changes in the mixture.

Pump Selection and Mass Flow Determination

The mass flow rate parameter, \dot{m} , is set by selection of a pump. To maintain constant \dot{m} across various experimental runs despite changing working fluid viscosity, power delivered to the pump must be reduced as the mixture mass fraction of water increases. To achieve this level of control, a variable DC power supply is used to drive the pump with input power reduced at lower working fluid viscosities.

Use of a fluid mixture instead of pure water suggested need to use a diaphragm pump to provide continuous flow while avoiding possible fouling or damage to internal components of a conventional rotary pump. The selected pump must provide adequate mass flow rate to access most of the laminar range considering Reynolds number for flow between circular flat plates [45],

$$0 < Re_m = \frac{\dot{m}_c}{\pi r_o \mu} < 2000 \quad (11)$$

To reach the upper laminar flow regime range, the working fluid mixture with lowest fluid viscosity (100% water) is used. The selected pump is a Seaflo 24.5-amp 12 VDC 53-Series diaphragm pump with nameplate capability to deliver 7.0 gallons-per-minute (26.5 liters-per-minute) at 60 PSI (413.7 kPa).

As described above, it is desirable to maintain constant \dot{m} as working fluid viscosity is varied across multiple experimental runs. To establish the fixed \dot{m} used in repeat experiment, the available pump mass flow rate as a function of fluid viscosity is determined gravimetrically by running fluid of increasing viscosity through the pump and weighing accumulation as a function of time. These data are then used to fit a predictive power function for the pump's performance that relates viscosity to maximum flow rate.

Since the purpose of this experiment is to explore the largest range of laminar Reynolds numbers, it is desirable to maximize the ratio $Re_{m,max}/Re_{m,min}$ where $Re_{m,max}$ is the Reynolds number for pure water at the mass flow rate fixed for the experiment, and $Re_{m,min}$ is the Reynolds number for the water/corn syrup mixture used to fix \dot{m} . The range of available

Reynolds numbers for the fluid mixture is bound by the range of mixture viscosities: $0.001 \frac{kg}{m-s} \text{ (water)} < \mu < 4.4 \frac{kg}{m-s} \text{ (corn syrup)}$.

It is recognized that the Reynolds number of Eq. (11) includes the outer disk radius, r_o , in the denominator. Re_m can be made arbitrarily large by making r_o smaller. However, there is a practical limit on the smallness of r_o , which is discussed in the next sub-section "Selection of Outer and Inner Disk Radii". Since for both $Re_{m,max}$ and $Re_{m,min}$ the parameters \dot{m}_c and r_o are the same, the ratio simplifies to a viscosity quotient,

$$\frac{Re_{m,max}}{Re_{m,min}} = \frac{\left(\frac{\dot{m}_c}{\pi r_o \mu}\right)_{max}}{\left(\frac{\dot{m}_c}{\pi r_o \mu}\right)_{min}} = \frac{\mu_{max}}{\mu_{min}} \quad (12)$$

The largest possible $Re_{m,max}/Re_{m,min}$ ratio within the constraints on \dot{m} and μ is determined by iteration. For the selected pump and binary fluid components the mass flow rate range is $0.0168 \frac{kg}{m-s} < \dot{m} < 0.025 \frac{kg}{m-s}$ which yields a Reynolds number ratio range of $202.8 < Re_{m,max}/Re_{m,min} < 392.5$.

While it is desirable to maximize $Re_{m,max}/Re_{m,min}$, access to the largest experimental space, it is also important to note two more factors: 1) where along the $\partial\eta/\partial Re_m$ curve [Fig. 1] the selected design point falls and 2) what power is being produced by the turbine at this design point.

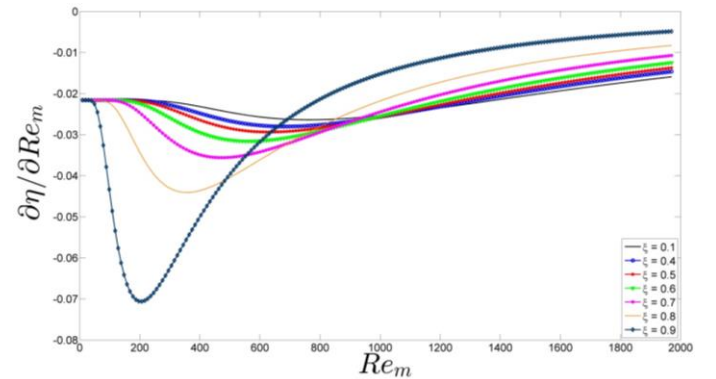


Figure 1: The derivative of turbine efficiency (dimensionless power) with respect to Re_m plotted for $0.1 = \xi$ and $0.4 < \xi < 0.9$ at 0.1 increments shows the derivative magnitude to be largest at $\xi = 0.9$ and $Re_m \approx 200$. This locus of maximized sensitivity corresponds to low turbine power output and is not a practical design point.

In the range $200 < Re_m < 800$, $|\partial\eta/\partial Re_m|$ is largest, which means the experiment is most sensitive to Reynolds number variations in this region: a desirable operational range when considered in isolation from the rest of the problem. However, large $|\partial\eta/\partial Re_m|$ only occurs for large ξ , which corresponds to turbine power output well below the established 0.5-Watt set point. Low power output is undesirable because the relative uncertainty in this measurement is fixed, making a small signal hard to discern from the noise.

Selection of Outer and Inner Disk Radii

The Tesla turbine performance embodied in Eq. (1) and Eq. (3) depends only on the dimensionless parameters Re_m^* and $\xi = r/r_o$. Therefore, the disk's outer and inner diameters can be set with some degree of flexibility subject to four constraints. First, r_o cannot be so small as to violate the restriction of Eq. (11) and cause $Re_m > 2000$, which would trip fluid to turbulence. While there is nothing physically preventing the flow from being turbulent, Eq. (1) upon which this entire analysis is predicated assumes laminar flow momentum transfer between the working fluid and disk. Thus, violating the laminar assumption invalidates this whole analysis. Considering other parameters already set, $r_o > 0.002$ m to keep the flow laminar. Second, small r_o necessitates high rotation rate to achieve power output at the 0.5 Watt range specified. If making r_o small, appropriate bearings must be found to support shaft rotation rates in excess of 25,000 rpm. Third, $\xi_i = r_i/r_o$ must be in a range that promotes strong turbine power sensitivity to Reynolds number (see Fig. 2) and high overall power output. As described elsewhere [13], these design needs are diametrically opposed. Thus, a compromise is struck by setting $\xi_i = 0.5$ to provide adequate power and sensitivity. Fourth, the inner diameter must be large enough to accommodate the central shaft, exhaust ports, and webbing material to hold the disks into the central shaft. It is this fourth restriction that ultimately sets the Tesla turbine's size, at least for this design process. The inner diameter is therefore selected at 0.02 m, providing a 4-cm-diameter space to fit everything.

Having set r_i and ξ_i , r_o becomes fixed at 0.04 m, yielding a 8-cm-diameter Tesla turbine.

Selection of Other Physical Parameters

The number of disks, disk spacing, and disk thickness remain to be set. As these parameters do not appear in the Tesla turbine performance model of Eq. (1) and Eq. (3) selection is guided by the literature. Rice [22] successfully used 2 mm-thick disks with 1 mm spacing. So those values are replicated. The minimum number of disks needed for system symmetry, 3, is selected to keep the experimental complexity low and the experiment physically small and manageable.

Bearing Selection & Turbine Material Selection

Given the selected parameters above, the turbine is expected to output 0.47 Watts, near the 0.50 Watt design specification. It will spin at just under 1200 rpm. With this information, bearings can be selected to hold the spinning shaft and disks inside the housing. A pair of VXB flanged sealed ceramic bearings housed in 304 stainless steel were selected. To prevent galvanic corrosion due to mismatching materials, 304 stainless steel will also be used for the turbine housing, axle, and disks.

RESULTS

Table 3 gives all the turbine parameters selected as a result of the design process described above. The experimentally

fixed mass flow rate of $\dot{m} = 0.025 \frac{kg}{s}$ gives $Re_{m,max} = 99.5$ [using an 88% corn syrup mass fraction, yielding $\mu_{max} = 0.203 \frac{kg}{m-s}$], and $Re_{m,min} = 0.49$ [using 100% water, yielding $\mu_{min} = 0.001 \frac{kg}{m-s}$]. The resulting ratio $Re_{m,max}/Re_{m,min} = 202.8$, and the expected power output is $\dot{W} = 0.47$ Watts. The turbine should deliver 0.024 mN-m torque at a rotation rate of $\omega_{max} = 1197$ rev/min.

DISCUSSION

Tesla turbine performance equations have been applied to enable a systematic design process achieving the goals of 1) creating a Tesla turbine where a single identified parameter, kinematic viscosity, can be easily varied to test its performance impact on the turbine while holding all other parameters fixed and 2) sizing the turbine to maximize sensitivity of varying kinematic viscosity making experimental measurement easier.

Table 3: Final geometric and fluid property parameters resulting from the design process.

Turbine Parameter	Selected Value
r_o – Outer Radius	0.04 m
r_i – Inner Radius	0.02 m
n_{disks} - # Disks	3
t – Disk Thickness	0.002 m
b – Disk Spacing	0.001 m
h – Nozzle Height	0.0005 m
\dot{m} – Mass Flow Rate	0.025 kg/s
μ_{max} – Maximum Viscosity	0.203 kg/m-s

This design technique can also be used to explore performance of other specialized Tesla turbines designed to achieve specific goals and outcomes. For example, it has been thought that reducing the size of Tesla turbines to the micro scale will improve their performance. This outcome contrasts observed performance reduction in axial aero-derivative when they are scaled down to the micro-scale and suggests the possibility that Tesla turbines could be successfully used for power generation in micro-electromechanical systems (MEMS). Moreover, since Tesla turbines are essentially a series of stacked, spaced disks they will be relatively easy to fabricate using established MEMS CMOS processes.

To predict how a MEMS scale Tesla turbine will perform, it is instructive to start with Eq. (1), distribute through the leading exponential term, and consolidate terms to give

$$\widehat{W}(\xi, Re_m^*) = \frac{1}{\xi} \left[\widehat{W}_o e^{\frac{24\xi^2}{Re_m^*}} + \frac{Re_m^*}{24} \left[1 - e^{\frac{24}{Re_m^*}(\xi^2-1)} \right] \right] \quad (13)$$

The dimensionless inner/outer diameter ratio is bounded $0 < \xi < 1$, and any arbitrary representative value in this range can be selected, $\xi = 0.1$. The key question is what happens to \widehat{W} when Re_m^* approaches 0; in other words, what is the trend in momentum transfer between the working fluid and the turbine disks as the turbine shrinks in size. Putting $Re_m^* \rightarrow 0$ into Eq. (13) yields

$$\widehat{W}(\xi = 0.1, Re_m^* \rightarrow 0) = \frac{1}{0.1} \left[\widehat{W}_o e^{\frac{24(0.1)^2}{0}} + \frac{0}{24} \left[1 - e^{\frac{24}{0}((0.1)^2 - 1)} \right] \right] \quad (14)$$

The last term in parentheses goes to zero, giving

$$\widehat{W}(\xi = 0.1, Re_m^* \rightarrow 0) = \frac{1}{0.1} \left[\widehat{W}_o e^\infty + \frac{0}{24} [1 - 0] \right] \quad (15)$$

Finally, the lead term in parenthesis with coefficient \widehat{W}_o goes to infinity.

$$\widehat{W}(\xi = 0.1, Re_m^* \rightarrow 0) = \frac{\widehat{W}_o e^\infty}{0.1} \quad (16)$$

While Re_m^* cannot literally reach 0 (without stopping the flow, the null solution), it can be driven to arbitrarily small values. What does this result mean for the effectiveness of fluid-disk momentum transfer? Recall that \widehat{W} is the velocity difference between the working fluid and the turbine disks. Higher \widehat{W} implies high velocity difference, which means high momentum transfer to the disks, increased turbine efficiency, and higher power output. In short, low Reynolds number corresponds to high Tesla turbine performance, suggesting MEMS Tesla turbines as an important new area for research exploration.

Without building a MEMS-scale Tesla turbine, it is nonetheless possible to use scaling laws with a macro-scale experimental turbine to explore MEMS-scale Tesla turbine performance and behavior. Using liquid working fluid in the macro-scale turbine and matching Re_m^* and ξ allows replication of a much smaller turbine running products of combustion. Consider the inlet conditions for the millimeter-scale aero-derived turbine in Epstein [46]. Products of combustion (modeled as air) enter the turbine at 4 atm and 1600 K. At this temperature and pressure, $\rho_{air} = 0.8815 \text{ kg/m}^3$ and $\mu_{air} = 5.88 \times 10^{-5} \text{ kg/m}\cdot\text{s}$. Epstein claims a working fluid mass flow rate of $1.8 \times 10^{-4} \text{ kg/s}$ [46]. For comparison, consider the Reynolds number obtained in the 8-cm-diameter Tesla turbine designed via the process above running Propylene Glycol working fluid.

$$Re_{m,8cm} = \frac{\dot{m}}{\pi n \mu r_o} = \frac{0.162 \frac{\text{kg}}{\text{s}}}{\pi(3)(0.004 \frac{\text{kg}}{\text{m}\cdot\text{s}})(0.04 \text{ m})} = 212.2 \quad (17)$$

Applying similarity arguments, a micro-turbine with the same ξ and Re_m as the 8-cm-diameter Tesla turbine should demonstrate the same efficiency (dimensionless power) output.

$$Re_{m,8cm} = Re_{m,MEMS} = \frac{\dot{m}}{\pi n \mu r_o} \quad (18)$$

Using similarity arguments to solve for the disk radius of a millimeter-scale Tesla turbine with products of combustion as working fluid gives

$$r_o = \frac{\dot{m}}{\pi n \mu Re_{m,MEMS}} = \frac{1.8 \times 10^{-4} \frac{\text{kg}}{\text{s}}}{\pi(3)(5.88 \times 10^{-5} \frac{\text{kg}}{\text{m}\cdot\text{s}})(212.2)} = 0.00153 \text{ m} \quad (19)$$

Thus, the characteristic disk radius of this millimeter-scale turbine with the same performance as the 8-cm-diameter Tesla turbine running Ethylene Glycol would be about 3 mm. That similarity-based characteristic diameter can be further driven down by increasing the working fluid pumping rate through the 8-cm-diameter turbine.

CONCLUSION

This paper applies analytical equations for turbine performance as the foundation to present a systematic Tesla turbine design process. To our knowledge, no Tesla turbine design process based in foundational theory has ever been published in the peer reviewed engineering literature. The process is shown to be flexible, allowing an engineering designer to select and address goals beyond simply maximizing turbine output power. This process was demonstrated in this paper by creating a Tesla turbine design where a single identified parameter, Reynolds number, can be easily varied to test its performance impact on the turbine while holding all other parameters fixed. The secondary goal of this design process is to size the turbine to maximize sensitivity to changes in Reynolds number to make experimental measurement more facile.

Reynolds number will be modulated at fixed working fluid mass flow rate using a two-component liquid mixture of water and corn syrup where kinematic viscosity is adjusted by changing the mass fraction of corn syrup. The turbine design results in 8 cm outer diameter and 4 cm inner diameter disks. The working fluid mass flow rate through the turbine is $\dot{m} = 0.025 \frac{\text{kg}}{\text{s}}$, giving a range of accessible Reynolds numbers from is $0.49 < Re_m < 99.5$ for a Reynolds number ratio of $Re_{m,max}/Re_{m,min} = 202.8$, more than two orders of magnitude increase and spanning the lower part of the laminar range. The turbine's expected power output is $\dot{W} = 0.47$ Watts with a delivered torque of 0.024 mN-m at a rotation rate of $\omega_{max} = 1197$ rev/min.

Combining the analytical equations underpinning the design process with similarity arguments, it is shown that shrinking the scale of a Tesla turbine drives the Reynolds number toward 0. The resulting velocity difference between the working fluid and the turbine disks gets driven toward infinity, which makes momentum transfer and the resulting turbine efficiency extremely high. In other words, unlike conventional turbines whose efficiency drops as they are scaled down, the

performance of Tesla turbines will increase as they are made smaller.

Finally, it is shown through similarity scaling arguments that the 8-cm-diameter turbine resulting from the design process of this paper running liquid Ethylene Glycol working fluids could be used to evaluate and approximate the performance of a 3-mm-diameter Tesla turbine powered by products of combustion.

NOMENCLATURE

b = Spacing between rotors
 h = Nozzle height
 \dot{m} = Mass flow rate through turbine
 \dot{m}_c = Mass flow rate in a channel between disk rotor pairs
 n_{disk} = Number of rotor disks
 r = Rotor radius
 r_i = Rotor radius at the turbine inlet (outer radius)
 r_o = Rotor radius at the turbine outlet (inner radius)
 Re_m = Reynolds number based on channel mass flow rate
 Re_m^* = Modified Reynolds number [$\frac{2b}{r_o} Re_m = Re_m^*$]
 $Re_{m,8cm}$ = Reynolds number for an 8-cm-diameter disk turbine
 $Re_{m,max}$ = Reynolds number for water at \dot{m} fixed for $Re_{m,min}$
 $Re_{m,MEMS}$ = Reynolds number for a MEMS-scale disk turbine
 $Re_{m,min}$ = Reynolds no. for viscous mixture at pump-limited \dot{m}
 t = Disk rotor thickness
 U_i = Rotor surface tangential velocity at $r = r_i$
 U_o = Rotor surface tangential velocity at $r = r_o$
 VBN_i = Viscosity blending number of component i
 $VBN_{mixture}$ = Viscosity blending number of the mixture
 $v_{\theta,i}$ = θ -direction (tangential) working fluid velocity at $r = r_i$
 $v_{\theta,o}$ = θ -direction (tangential) working fluid velocity at $r = r_o$
 \dot{W} = Turbine mechanical output power
 $\hat{W}(\zeta, Re_m^*)$ = Dimensionless tangential velocity difference between the disk rotor & working fluid ($v_{\theta,i} - U$)/ U_o at any radial location
 \hat{W}_i = Dimensionless tangential velocity difference at $r = r_i$
 \hat{W}_o = Dimensionless tangential velocity difference at $r = r_o$
 Γ = Torque
 η = Turbine energy conversion efficiency
 μ = Working fluid dynamic viscosity
 μ_{air} = Dynamic viscosity of air
 μ_{max} = Viscosity of the most viscous 2-component working fluid
 μ_{min} = Viscosity of water (least viscous 2-component working fluid)
 ν_i = Dynamic viscosity of component i
 $\nu_{mixture}$ = Dynamic viscosity of the mixture
 ζ = Dimensionless radial coordinate = r/r_o
 ζ_i = Dimensionless radius ratio = r_i/r_o
 ρ_{air} = Density of air
 ω = Angular velocity (rad/sec)
 ω_{max} = Maximum angular velocity (rad/sec)

ACKNOWLEDGMENTS

We acknowledge in-kind donations of materials and volunteer time by Engineer Inc, a Tennessee-based engineering education technology company. Engineer Inc creates

inexpensive teaching laboratory equipment for engineering courses: www.engineerinc.net.

This paper's undergraduate authors are members of the Tennessee Undergraduate Researcher Network (TURN) at TSU, an organization that fast-tracks undergraduates into meaningful early research experiences. This project demonstrates the Undergraduate Researcher Incubator Hypothesis [47, 48].

REFERENCES

- [1] Jacobson, R., "Tesla Bladeless Pumps and Turbines," *Proceedings of the 26th Intersociety Energy Conversion Engineering Conference*, Vol. 4, Piscataway, NJ, 1991, pp. 445-450.
- [2] Wakeman, T., Tabakoff, W., "Turbomachinery Affected by Environmental Solid Particles," Paper 79-0041, *Proceedings of the 17th AIAA Aerospace Sciences Meeting*, New Orleans, LA, January 15-17, 1979.
- [3] Grant, G., Tabakoff, W., "Erosion Prediction in Turbomachinery Resulting from Environmental Solid Particles," *AIAA Journal of Aircraft*, Vol. 12, May 1975, pp. 471-478.
- [4] Ghenaïet, A., "Study of Particle Ingestion through Two-Stage Gas Turbine," Paper GT2014-25759, *Proceedings of the ASME Turbine Technical Conference and Exposition*, Vol. 2C, Düsseldorf, Germany, June 16-20, 2014.
- [5] Tabakoff, W., Hamed, A., Metwally, M., "Effect of Particle Size Distribution on Particle Dynamics and Blade Erosion in Axial Flow Turbines," *Journal of Gas Turbine and Power*, Vol. 113, Oct. 1991, pp. 607-615.
- [6] Rice, W., "Tesla Turbomachinery," *Proceedings of the 4th International Tesla Symposium*, Serbian Academy of Sciences and Arts, Belgrade, Yugoslavia, Sept. 22-25, 1991.
- [7] Gupta, H. E., Kodali, S. P., "Design and Operation of Tesla Turbo Machine - A State of the Art Review," *International Journal of Advanced Transport Phenomena*, Vol. 2, No. 1, 2013 pp. 7-14.
- [8] Tahil, W., "Theoretical Analysis of a Disk Turbine," *Tesla Engine Builder's Association (TEBA) Newsletter*, Vol. 15, 1998, pp 18-19.
- [9] Tahil, W., "Theoretical Analysis of a Disk Turbine (2)," *Tesla Engine Builder's Association (TEBA) Newsletter*, Vol. 16, 1999, pp 15-16.
- [10] Carey, V. P., "Assessment of Tesla Turbine Performance for Small Scale Solar Rankine Combined Heat and Power Systems," *Journal of Engineering for Gas Turbines and Power*, Vol. 132, No.3, pp. 122301-1 - 122301-8.
- [11] Carey, V. P., "Assessment of Tesla Turbine Performance for Small Scale Solar Rankine Combined Heat and Power Systems," IMECE2009-10814, *Proceedings of the 2009 ASME International Mechanical Engineering Congress & Exposition*, Lake Buena Vista, Florida, November 13-19, 2009.
- [12] Krishnan, V. G., Romanin, V., Carey, V. P., Maharbiz, M. M., "Design and scaling of microscale Tesla turbines," *Journal of Micromechanics and Microengineering*, Vol. 23, 2013.

- [13] Traum, M. J., Hadi, F., Akbar, M. K., "Extending 'Assessment of Tesla Turbine Performance' Model for Sensitivity-Focused Experimental Design," *ASME Journal of Energy Resources Technology*, Submitted, 2017.
- [14] Fréchette, L. G., Lee, C., Arslan, S., Liu, Y. C., "Design of a microfabricated Rankine cycle steam turbine for power generation," IMECE2003-42082, *Proceedings of the 2003 ASME International Mechanical Engineering Congress and Exposition*, Washington, DC, November 15–21, 2003, pp. 335-344.
- [15] Epstein, A. H., "Millimeter-scale, micro-electromechanical systems gas turbine engines," *ASME Journal of Engineering for Gas Turbines and Power*, Vol. 126, No. 2, 2004, pp. 205–226.
- [16] Lee, C., Fréchette, L. G., "A silicon microturbopump for a rankine-cycle power generation microsystem—Part I: Component and system design," *Journal of Microelectromechanical Systems*, Vol. 20, No. 1, 2011, pp. 312-325.
- [17] McKeathen, J. E., Reidy, R. F., Boetcher, S. K., Traum, M. J., "A Cryogenic Rankine Cycle for Space Power Generation," Paper Number 2009-4247, *Proceedings of the 41st AIAA Thermophysics Conference*, San Antonio, TX, June 22 - 25, 2009.
- [18] Tesla, N, United States of America Patent 1,061,206, 1913.
- [19] Swithenbank, A. M. "The Tesla Boundary Layer Turbine," Web URL: <http://www.stanford.edu/~hydrobay/lookat/tt.html>, accessed 3/13/2017.
- [20] Boyd, K. E., Rice, W., "Laminar Inward Flow of an Incompressible Fluid Between Rotating Disks With Full Peripheral Admission," *Journal of Applied Mechanics*, Vol. 35, No. 2, 1968, pp 229-237.
- [21] Matsch, L., Rice, W., "An Asymptotic Solution for Laminar Flow of an Incompressible Fluid Between Rotating Disks," *Journal of Applied Mechanics*, Vol. 35, No. 1, 1968, pp. 155-159.
- [22] Rice, W., "An Analytical and Experimental Investigation of Multiple-Disk Turbines," *Journal of Engineering for Power, Transactions of the ASME*, Vol. 87, No. 1, 1965, pp. 29-36.
- [23] Lawn, M. J., Rice, W., "Calculated Design Data for the Multiple-Disk Turbine Using Incompressible Fluid," *Journal of Fluids Engineering*, Vol. 96, No. 3, 1974, pp. 252-258.
- [24] Truman, C. R., Rice, W., Jankowski, D. F., "Laminar Throughflow of Varying-Quality Steam Between Corotating Disks," *Journal of Fluids Engineering*, Vol. 100, No. 2, 1978, pp. 194-200.
- [25] Hoya, G. P., Guha, A., "The design of a test rig and study of the performance and efficiency of a Tesla disc turbine," *Proceedings of the Institution of Mechanical Engineers, Part A: Journal of Power and Energy*, Vol. 223, No. 4, 2009, pp. 451-465.
- [26] Guha, A., Sengupta, S., "Similitude and scaling laws for the rotating flow between concentric discs," *Proceedings of the Institution of Mechanical Engineers, Part A: Journal of Power and Energy*, Vol. 228, June 2014, pp. 429-439.
- [27] Deng, Q., Qi, W., Feng, Z., "Improvement of a Theoretical Analysis Method for Tesla Turbines," GT2013-95425, *2013 ASME Turbo Expo*, San Antonio, TX, June 3–7, 2013.
- [28] Qi, W., Deng, Q., Feng, Z., Yuan, Q., "Influence of Disc Spacing Distance on the Aerodynamic Performance and Flow Field of Tesla Turbines," GT2016-57971, *2016 ASME Turbo Expo*, Seoul, South Korea, June 13–17, 2016.
- [29] Guha, A., Sengupta, A., "The fluid dynamics of work transfer in the non-uniform viscous rotating flow within a Tesla disc turbomachine," *Physics of Fluids*, Vol. 26, 2014.
- [30] Yang, Z., Weiss, H. L., Traum, M. J., "Gas Turbine Dynamic Dynamometry: A New Energy Engineering Laboratory Module," *Proceedings of the 2013 American Society for Engineering Education North Midwest Section Conference*, Fargo, North Dakota, October 17-18, 2013.
- [31] Yang, Z., Weiss, H. L., Traum, M. J., "Dynamic Dynamometry to Characterize Disk Turbines for Space-Based Power," *Proceedings of the 23rd Annual Wisconsin Space Conference*, Milwaukee Wisconsin, August 15-16, 2013.
- [32] Usman, M., Khan, S., Ali, E., Maqsood, M. I., Nawaz, H., "Modern improved and effective design of boundary layer turbine for robust control and efficient production of green energy," *Journal of Physics: Conference Series*, Vol. 439, 2013.
- [33] Beans, E. W. "Performance Characteristics of a Friction Disk Turbine," Doctoral Dissertation, Pennsylvania State University, 1961.
- [34] Leaman, A. B. "The Design, Construction and Investigation of a Tesla Turbine," Master's Thesis, University of Maryland, 1950.
- [35] Gupta, E. H., Kodali, S. O., "Design and Operation of Tesla Turbo machine - A state of the art review," *International Journal of Advanced Transport Phenomena*, Vol. 2, No. 1, 2013
- [36] Lampart, P., Jędrzejewski, Ł., "Investigations of Aerodynamics of Tesla Bladeless Microturbines," *Journal of Theoretical and Applied Mechanics*, Vol. 49, No. 2, 2011, pp. 477-499.
- [37] Pandey, R. J., Pudasaini, S., Dhakal, S., Uprety, R. B., Neopane, H. P., "Design and Computational Analysis of 1 kW Tesla Turbine," *International Journal of Scientific and Research Publications*, Vol. 4, Issue 11, 2014.
- [38] Romanin, V. D., Krishnan, V. G., Carey, V. P., Maharbiz, M. M., "Experimental and Analytical Study of Sub-Watt Scale Tesla Turbine Performance," IMECE2012-89675, *Proceedings of the 2010 ASME International Mechanical Engineering Congress and Exposition*, Houston, TX, November 9–15, 2012, pp. 1005-1014.
- [39] Wee, T., Rahman, A. A., Shy, J. F., Eng, A. L., "Optimization of Tesla turbine using Computational Fluid Dynamics approach," *Proceedings of the 2011 IEEE Symposium on Industrial Electronics and Applications*, 2011, pp. 477-480.
- [40] Ho-Yan, B. P., "Tesla turbine for pico hydro applications," *Guelph Engineering Journal*, Vol. 4, 2011, pp. 1-8.
- [41] Cross, N., Engineering Design Methods – Strategies for Product Design, 4th Edition, Wiley, 2008.

- [42] Hasan, A., Benzamia, A., "Investigating the Impact of Air Temperature on the Performance of a Tesla Turbine Using CFD Modeling," *International Journal of Engineering Innovation & Research*, Vol. 3, Issue 6, 2014, pp 794-802.
- [43] Maples, R. E., Petroleum Refinery Process Economics, 2nd Edition, Pennwell Books, 2000.
- [44] Chirife, J., Buera, M. P., "A simple model for predicting the viscosity of sugar and oligosaccharide solutions," *Journal of Food Engineering*, Vol. 33, No. 3-4, 1997, pp. 221-226.
- [45] White, F. M., Fluid Mechanics, 7th Edition, McGraw Hill, 2011, p. 382.
- [46] Epstein, A. H. "Millimeter-scale, MEMS gas turbine engines," *Proceedings of the 2003 ASME International Joint Power Generation Conference*, 2003.
- [47] Traum, M. J., Karackattu, S. L. Houston Jackson, D., McNutt, J. D., "Organization to Fast-Track Undergraduate Students Into Engineering Research via Just-In-Time Learning," *Proceedings of the Conference On Being an Engineer: Cognitive Underpinnings of Engineering Education*, Lubbock, TX, February 1-2, 2008.
- [48] Traum, M. J., Karackattu, S. L., "The Researcher Incubator: Fast-tracking Undergraduate Engineering Students into Research via Just-in-Time Learning," Paper Number 09-33, *Proceedings of the 2009 ASEE Gulf-Southwestern Section Annual Conference*, Waco, TX, March 18 – 20, 2009.